

## Interaction of hydrogen $H_n^+$ clusters with thin carbon foils

M. Farizon, N. V. de Castro Faria,\* B. Farizon-Mazuy, and M. J. Gaillard

*Institut de Physique Nucléaire (and IN2P3), Université Claude Bernard Lyon I, 43 boulevard du 11 Novembre 1918, 69622 Villeurbanne CEDEX, France*

(Received 18 July 1991)

A Monte Carlo computer program was developed to calculate the angular distribution of fragments resulting from the breakup of fast hydrogen clusters  $H_n^+$  when traversing thin amorphous carbon foils. The three-dimensional relative coordinates of each proton in the cluster are given as input. The code begins with a generation of a random orientation of clusters. Next, the foil is divided into slabs and the effects of Coulomb explosion, multiple scattering, and energy loss on each fragment are calculated for successive slabs. The distributions of separations and relative velocities at the exit surface as well as the angular distributions of fragments are then obtained. Therefore, the cluster-stopping-power ratio is given. The use of the code is illustrated in the case of 30-, 40-, 60-, and 80-keV/ $p$  clusters, with  $n=2, 3$  to 21 odd, impinging on a  $2\text{-}\mu\text{g}/\text{cm}^2$  carbon foil, where experimental results are available.

PACS number(s): 34.10.+x, 34.50.Bw, 36.40.+d

### I. INTRODUCTION

The penetration of clusters with energies ranging from 25 keV/atom to a few MeV/atom has received considerable interest in connection with charge-exchange processes, convoy-electron, secondary-electron production in ion-solid interactions, etc. While the interaction of atomic particles with solid matter has been studied in great detail, the study of cluster interactions is still in its initial phase. Hydrogen clusters are of special interest, for both the experimental and the theoretical point of view, because of their relative simplicity. In recent works [1,2] we have reported on measurements of angular distributions of hydrogen fragments resulting from the dissociation of fast  $H_n^+$  clusters ( $n \leq 21$ , odd) in a carbon foil. The proximity effects on the fragment neutralization has accordingly been investigated. These results have motivated the development of a Monte Carlo computer routine to allow a quantitative treatment of the different processes involved in the interaction of the cluster with the solid. In the attempt to interpret this increasing number of experimental results already available, and looking for the possibilities that will be opened with faster clusters [3], it is necessary to analyze the implications of models currently employed for molecular ions [4–6], and to consider more complex situations. Otherwise, as the complexity of calculations increases, the difficulties of analytical methods tend to rise more sharply than those of numerical methods. Monte Carlo simulation is a numerical method that is very well suited to the kind of situation that we are dealing with, i.e., Coulomb explosion, classical trajectories, etc.

### II. THE MONTE CARLO ROUTINE

A computer program based on a Monte Carlo procedure has been developed to evaluate the trajectories of a molecular-projectile ion inside the solid. To obtain conclusive results in view of the statistical nature of processes

such as multiple scattering, the history of 1000–10 000 cluster ions is calculated. Our model assumes the following sequence of events.

(i) The incident  $H_n^+$  cluster with a known structure is initially randomly oriented relative to the incident beam direction. The cluster is assumed to dissociate upon contact with the foil. Bombarding clusters are assumed to be three-dimensional with a structure calculated by *ab initio* methods.

(ii) The motion of the fragments inside the solid is treated classically. The foil is divided into a large number of thin parallel slabs. The program treats the nuclear scattering in each slab as a single event where each cluster fragment can change direction and then proceeds on its way until the next collision. From the  $n$ th to the  $(n+1)$ th slab, the calculation of the particle trajectories takes into account the electronic energy loss, the influence of the superposed wake potentials, and the screened Coulomb explosion. The process is repeated  $n$  times until the fragments reach the exit surface of the foil. Then, all interesting parameters such as the internuclear separation  $R_{ij}$  between the protons  $i$  and  $j$ , the velocity  $v$ , and the flight directions of each fragment are stored. A large number of cluster ions are followed through the foil according to this procedure. Distributions of interatomic separation and relative velocities are then obtained in the form of histograms. In the following paragraphs we will describe the assumptions made in the calculations.

#### A. Initial structure and orientations of the $H_n^+$ cluster ions

The three-dimensional structures of the incident cluster ions have been calculated by *ab initio* methods [7,8]. Using triple-zeta-plus-polarization basis sets, self-consistent-field calculations have been carried out for  $H_n^+$ ,  $n=2-21$ , odd. Initial relative velocities of protons in the cluster are ignored. This will be discussed later. In

all cases we assume a random distribution of the initial orientation of the cluster structure.

### B. Coulomb explosion

When a cluster penetrates into a solid it loses its binding electrons after a few atomic layers. Then the cluster fragments repel each other by their mutual Coulomb repulsion ("Coulomb explosion"). The repulsion starts with the bond length  $R_{ij}^0$  of the protons of the cluster which are  $R_{ij} = 0.89, 1.66, 0.75$  Å in the case of the  $H_9^+$  ion, for example [7]. The interacting electrons inside the solid can be treated as a free-electron gas and we assume that the potential  $V_{ij}$  between two fragments  $i$  and  $j$  of the cluster is exponentially screened with a screening length  $a = v/\omega_p$  [8]. Here  $v$  is the projectile velocity and  $\omega_p$  the plasma frequency of the solid. We also assume a charge-exchange equilibration in the foil and we use the concept of an "effective charge" discussed by Brandt [9]. The effective charge  $Z_{\text{eff}}$  has been taken from Ref. [10]. It is assumed that the  $Z_{\text{eff}}$  of each fragment is the same as in the atomic case. The effect of this "explosion" is obtained by numerically integrating the classical equations of motion between scattering events. For a given target thickness  $x$  the "Coulomb explosion" results in constant internuclear separations at the exit of the foil. When multiple scattering is included one obtains a distribution  $F(R_{ij})$  of internuclear separations.

### C. Nuclear scattering

The predominant effect of the scattering of the fragments by target nuclei as they traverse the foil is to cause a change in direction. Nuclear scattering also causes a small energy loss. The scattering cross section resulting from a Thomas-Fermi-type screened Coulomb potential [9] is used for the calculation of these effects. The polar scattering angles are chosen from distributions derived from this cross section. The azimuthal scattering angle is randomly distributed in the  $2\pi$  interval. The scattering cross section is assumed to be constant for the total flight path of the cluster ion. The change in the energy-dependent cross section caused by the energy loss inside the foil is not taken into account. Test calculations of the multiple-scattering distributions are in good agreement with values tabulated in Ref. [11]. We assume that the fragments of a cluster are independent with respect to the nuclear scattering [12].

### D. Energy loss—wake potential

Interactions between a projectile ion and a target result in energy loss of the ion. At intermediate projectile energy ( $25 \text{ keV}/p \leq E \leq 100 \text{ keV}/p$ ), the excitations and ionizations induced in the target affect mostly the very loosely bound valence electrons. Thus it is possible to describe the medium of the interacting electrons like a free-electron gas with a dielectric function  $\epsilon$  [13,14].

Let us consider a cluster of  $N$  charges  $Z_i$  and relative positions  $\mathbf{R}_{ij}$  moving with nonrelativistic velocity  $\mathbf{v}$  in a material medium of longitudinal dielectric constant

$\epsilon(\mathbf{k}, \omega)$ . A general expression for the energy loss per unit time of such a cluster in this medium is given by

$$\frac{dW}{dt} = \frac{-e^2}{2\pi^2} \int d^3k \frac{\mathbf{k} \cdot \mathbf{v}}{k^2} \text{Im} \left[ \frac{-1}{\epsilon(\mathbf{k}, \mathbf{k} \cdot \mathbf{v})} \right] \times \left[ \sum_i Z_i^2 + \sum_{i \neq j} Z_i Z_j \cos(\mathbf{k} \cdot \mathbf{R}_{ij}) \right],$$

where the terms with  $i=j$  give the energy loss of totally independent charges and the terms with  $i \neq j$  represent interference effects on the energy loss due to the simultaneous perturbation of the medium by the charges in correlated motion. For the present calculations the dielectric function  $\epsilon$  is

$$\epsilon(\mathbf{k}, \omega) = 1 + \omega_p^2 \left[ \beta^2 k^2 + \frac{\hbar^2 k^4}{4m^2} - \omega(\omega + i\gamma) \right]^{-1}.$$

The constant  $\beta = (\frac{3}{5})^{1/2} v_F$  describes the propagation of density distortions in an electron gas,  $v_F$  is the Fermi velocity of electrons in the medium, and  $\gamma$  is the damping. The charges  $Z_i$  and  $Z_j$  are assumed to be the effective charge used in the "Coulomb explosion" calculation. Due to the amount of computer time involved in such calculation, the energy loss is not included in all the calculations of the velocities and distances distributions. The energy-loss effect on the full width at half maximum (FWHM) of the velocity distributions calculated with  $H_n^+$  clusters at 60 keV/ $p$  is about 3%.

## III. RESULTS

In previous publications [1,2] we have reported on measurements of angular distributions of hydrogen fragments resulting from the dissociation of fast  $H_n^+$  clusters ( $n=2$  to 21, odd) in a carbon foil. The proximity effects have been investigated for beam velocities above the Bohr velocity and it had been observed at a given velocity that the angular width "saturates" at  $n \geq 5$ . The angular distribution reflects mainly the combined effects of multiple scattering and screened Coulomb explosion in the foil since it is quite reasonable to assume that the repulsion in vacuum of a neutral fragment with either other protons or neutral fragments is negligible. As an illustration we show in Fig. 1 the angular distributions of the  $H^0$  fragments resulting from the dissociation of  $10^4 H_9^+$  clusters (60 keV/ $p$ ) in a carbon foil of thickness  $2 \mu\text{g}/\text{cm}^2$ . The solid curve and the points represent the angular distributions obtained by computation and experiment, respectively. Our calculation reproduces quantitatively the experimental results.

In Fig. 2 the variation of the FWHM of the angular distribution of neutrals  $H^0$  emerging from a carbon foil ( $2 \mu\text{g}/\text{cm}^2$ ) as a function of the mass number  $n$  of the incident clusters is presented for various projectile velocities. The dark points and open points represent experimental and calculated results, respectively. A good agreement is observed for  $n \geq 5$ . Nevertheless, for the case of  $H_2^+$  and  $H_3^+$  incident ions, the computed values are too large. As the calculation is good for the proton case ( $n=1$ ), this overestimated effect comes from the

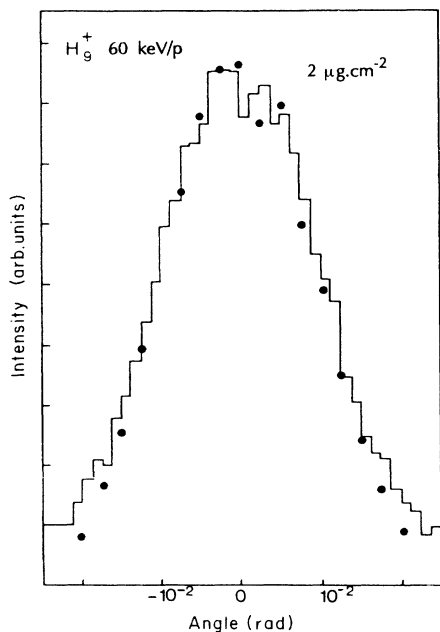


FIG. 1. Angular distribution of emerging fragments resulting from the collision of 60-keV/p  $H_9^+$  clusters with a  $2\text{-}\mu\text{g}/\text{cm}^2$  carbon foil. The filled circles are measurements from Ref. [1]. The solid line is the result of Monte Carlo calculations.

Coulomb explosion calculation which is strongly dependent on the initial internuclear distances in the cluster.

Indeed, a central part of the analysis of such experiments is the knowledge of the distribution of internuclear separations of the clusters in the incident beam. For example, it has been shown that  $\text{HeH}^+$  ions produced in a rf source were vibrationally "hotter" than those produced in a duoplasmatron source [15]. In our case, the

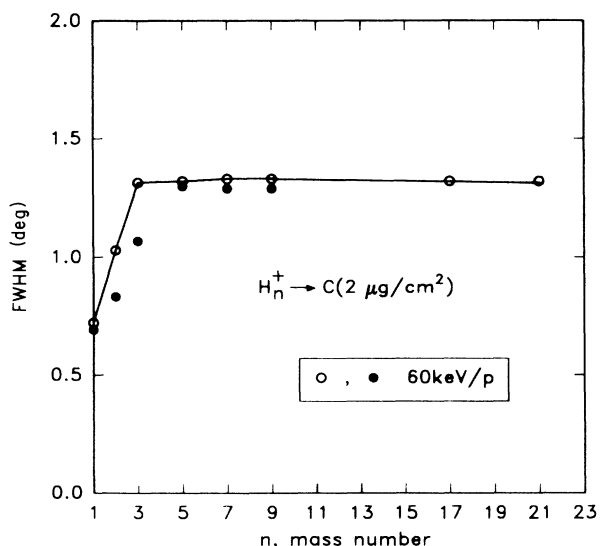


FIG. 2. Variation with the cluster mass number  $n$  of the FWHM of the angular distribution of  $H^0$  atoms emerging from a  $2\text{-}\mu\text{g}/\text{cm}^2$  carbon foil at a velocity of 60 keV/p. The open symbols correspond to calculated results. The filled symbols correspond to experimental results.

repulsion calculation starts with the bond lengths  $R_{ij}^0$  of the cluster being calculated by an *ab initio* method. These internuclear separations are  $R_{H_3^+}^0 = 0.85 \text{ \AA}$  and  $R_{H_2^+}^0 = 0.65 \text{ \AA}$ . Let the values  $R_{ij}^0$  for  $H_3^+$  and  $H_2^+$  cases have a probability distribution  $D(R_{ij}^0)$  which depends on the population of the various vibronic states of the projectile [15]. To fit the data, the only adjustable parameters are the most probable value of  $R_{ij}^0$  and the standard deviation  $\sigma_{ij}$  of the distribution  $D(R_{ij}^0)$  assumed here to be Gaussian. At 60-keV/p energy, the best fit is obtained for  $\bar{R}_{H_3^+}^0 = 1.2 \text{ \AA}$  with  $\sigma_{H_3^+} = 0.2 \text{ \AA}$  and  $\bar{R}_{H_2^+}^0 = 1.3 \text{ \AA}$  with  $\sigma_{H_2^+} = 0.4 \text{ \AA}$  (see Fig. 3). A good agreement with the experimental data is also obtained with these initial-distance distributions at the other energies (Fig. 3).

The results concerning cluster mass numbers higher than 3 are quantitatively in good agreement with the initial bond lengths calculated by *ab initio method*. This means that the bombarding clusters are in such vibrational states that the vibrations both of the  $H_3^+$  core and of the  $H_2$  subunits are not involved. Hydrogen-cluster structure is a nucleation of  $H_2$  molecules around a  $H_3^+$  core and these clusters are weakly bound. Even if clusters with a  $H_3^+$  core and  $H_2$  subunits in a high vibrational state are produced in the cluster ion source, these results show that most of them must have dissociated before the mass analysis of the beam (the time of flight between the cluster source and the beam analyzer is about 3  $\mu\text{s}$ ). We have also calculated the FWHM of the distribution of the fragments after dissociation of  $H_2$  molecules at 60 keV/p with an initial structure obtained by the *ab initio* method. We have obtained a FWHM of  $1.17^\circ$  which is close to the  $H_3^+$  value ( $1.31^\circ$ ) but smaller. Concerning the clusters, the ratio of the number of protons in a  $H_2$

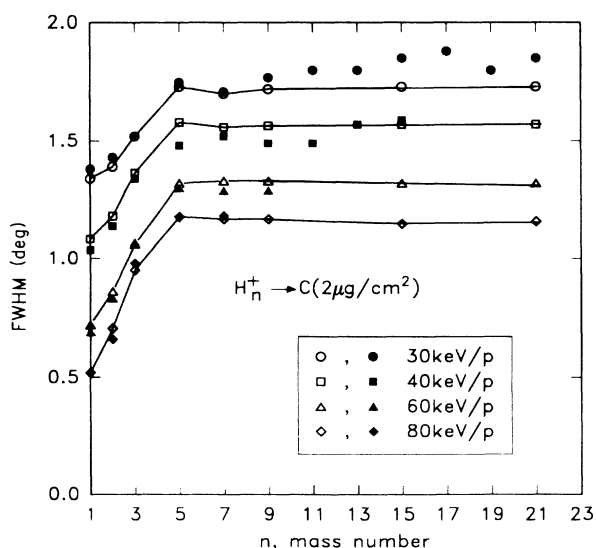


FIG. 3. Variation with the cluster mass number  $n$  of the FWHM of the angular distribution of  $H^0$  atoms emerging from a  $2\text{-}\mu\text{g}/\text{cm}^2$  carbon foil for various projectile velocities. The open symbols correspond to calculated results. The filled symbols correspond to experimental results.

subunit to the number of protons in the  $H_3^+$  core grows fast with the size of the cluster. So, one could expect a decrease of the FWHM of the fragment distribution with the increase of the cluster size until one reaches the  $H_2$  value. The experimental data and the calculated results show that the FWHM value does not change significantly from  $n=5$  to 21. This shows that, even if the  $H_3^+$  core and the  $H_2$  subunits are not very closed, the  $H_3^+$  core increases the repulsion between the protons of the  $H_2$  subunits.

We can also predict the cluster-stopping-power ratio for various mass numbers. Due to the increasing computer time, we did not perform the calculation of the cluster-stopping-power ratio for mass numbers greater than 9 and have neglected the energy straggling. Kemmler *et al.* [6] have shown that, for  $N_2^+$  ions at energies between 25 and 100 keV/amu on a carbon target, the cluster-stopping-power ratio increases by less than 10% when including energy straggling. Figure 4 presents the calculated cluster-stopping-power ratio  $R_s$  for  $H_n^+$  ions on a  $2\text{-}\mu\text{g}/\text{cm}^2$  carbon target at 60 keV/ $p$  velocity for various mass numbers ( $n=2,3$  to 9, odd). The  $H_2^+$  experimental results of Eckart *et al.* [16] are also presented in Fig. 4. This result was obtained with  $H_2^+$  ions at 60 keV/ $p$  with a  $3\text{-}\mu\text{g}/\text{cm}^2$  carbon foil. One notes that the results of Eckart *et al.* are a little bit below our results, as expected, since the target used is thicker. It is interesting to note that at the velocity studied (greater than Bohr velocity), the stopping power ratio is larger than one and “saturates” for  $n \geq 5$  mass number. The stopping power obtained with cluster beams at 60 keV/ $p$  impinging on a  $2\text{-}\mu\text{g}/\text{cm}^2$  carbon foil is about 20%

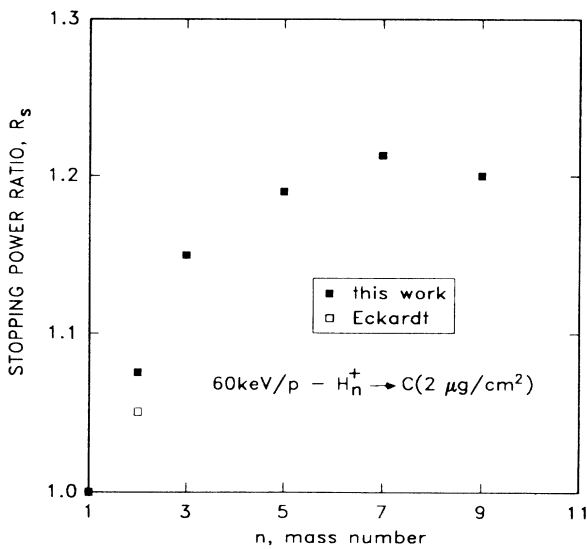


FIG. 4. Stopping power ratio  $R_2 = [dE(H_n^+)/dx] / ndE(H^+)/dx$  resulting from the passage of 60-keV/ $p$   $H_n^+$  (clusters ( $n=2,3$  to 9, odd) through a  $2\text{-}\mu\text{g}/\text{cm}^2$  carbon foil as a function of the cluster mass number. The filled symbols correspond to the calculated results. The open symbol corresponds to the experimental value obtained by Eckardt *et al.* [16].

greater than the proton case. As for the angular distribution results, a saturation effect should be observed due to the structure of the incident cluster ions at the entrance of the target, i.e., the small distances between the protons at the entrance of the foil.

Computed internuclear separation distributions at the exit of the foil for incident  $H_n^+$  ( $n=2, 3$  to 21, odd) at an energy of 60 keV/proton and for C foils of thickness  $2\text{ }\mu\text{g}/\text{cm}^2$  are presented in Fig. 5. We have also computed the internuclear-separation distribution resulting from the traversal of 0.2 MeV/proton  $H_2^+$  ions through  $6\text{-}\mu\text{g}/\text{cm}^2$  carbon foils and our results are in good agreement with the Schectman results [4]. In Fig. 5 each distribution presents various typical distances  $R_{ij}$  which are representative of small and large distances between atoms

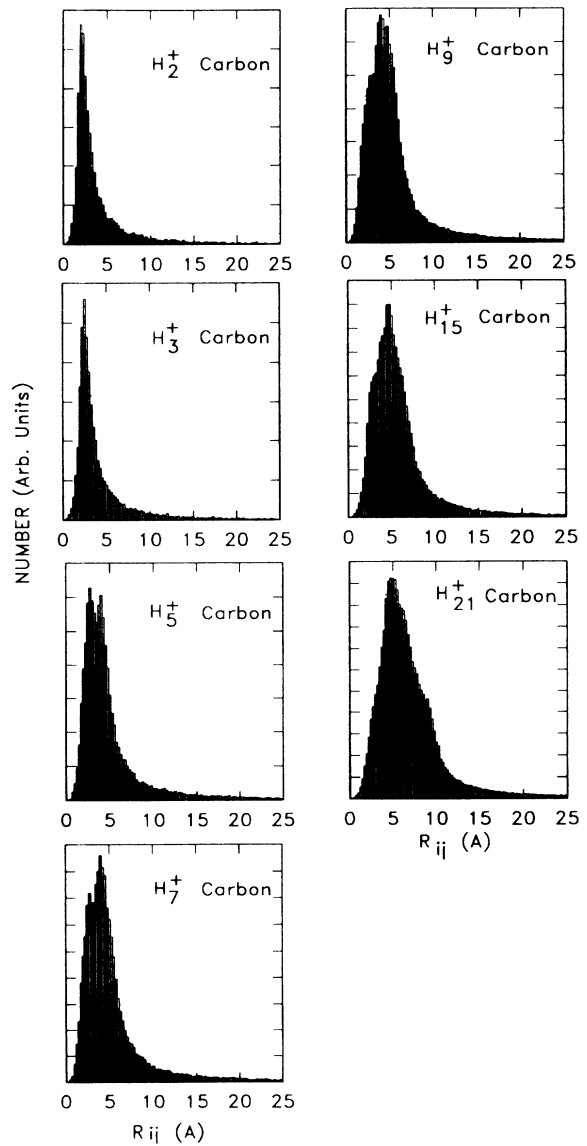


FIG. 5. Calculated internuclear separation distributions  $F(R_{ij})$  resulting from the passage of 60-keV/ $p$   $H_n^+$  clusters ( $n=2,3$  to 21, odd) through  $2\text{-}\mu\text{g}/\text{cm}^2$  carbon foil.

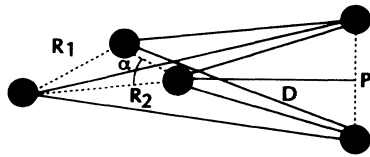


FIG. 6. The initial structure of the  $H_5^+$  cluster. The dotted lines correspond to the small distances and the solid lines correspond to the large distances.

in the incident cluster. For example, in Fig. 6, the  $H_5^+$  structure corresponding to the bond lengths  $R_1=0.99 \text{ \AA}$ ,  $R_2=0.81 \text{ \AA}$ ,  $D=1.25 \text{ \AA}$ , and  $P=0.77 \text{ \AA}$  is represented. Due to multiple scattering, at the exit surface only two peaks in the distance distribution are observed. These two peaks are representative of the smaller distances and the larger distances corresponding to the dotted lines and the solid lines in Fig. 6, respectively. These results are at the root of the interpretation of the collective effect observed on charge exchange which is connected to the distances between the fragments at the exit of the foil.

#### IV. CONCLUSION

The interaction of three-dimensional hydrogen clusters with thin carbon targets has been simulated at incident energies of 30–80 keV/ $p$  for various mass numbers of the incident clusters. Due to the weakly bound states of the hydrogen clusters, in experiments where the analysis of the fast ionic clusters is done far from the source, the incident ions reach the foil in low vibrational states. Our results show that the effects observed with ionic hydrogen cluster beams are of the same magnitude as the effects which would be obtained with molecular beams of  $H_3^+$  and  $H_2$  in their fundamental state. We have also studied the cluster stopping power at velocities greater than the Bohr velocity. We have obtained an enhancement with respect to the proton case with the increase of the cluster size, but this effect does not change significantly from  $n=5$  to 9. Our simulation can also give the distances between the fragments at the exit of the foil and is an important tool for building a model on charge-exchange processes with cluster ions.

\*Permanent address: Pontifica Universidade Catolica do Rio de Janeiro, 22453 Rio de Janeiro, Brazil.

- [1] B. Mazuy, A. Belkacem, M. Chevallier, M. J. Gaillard, J. C. Poizat, and J. Remillieux, Nucl. Instrum. Methods Phys. Res. B **28**, 497 (1987).
- [2] M. Farizon, A. Clouvas, N. V. de Castro Faria, B. Farizon-Mazuy, M. J. Gaillard, E. Gerlic, A. Denis, J. Desesquelles, and Y. Ouerdane, Phys. Rev. A **43**, 121 (1991).
- [3] M. Chevallier, N. V. de Castro Faria, B. Farizon-Mazuy, M. J. Gaillard, J. C. Poizat, and J. Remillieux, J. Phys. C **2**, 189 (1989).
- [4] R. Schectman and W. D. Ruden, Nucl. Instrum. Methods Phys. Res. B **194**, 295 (1982).
- [5] D. Zajfman, G. Both, E. P. Kanter, and Z. Vager, Phys. Rev. A **41**, 2482 (1990).
- [6] J. Kemmler, P. Koschar, M. Burkhard, and K. O. Groeneveld, Nucl. Instrum. Methods Phys. Res. B **12**, 62 (1985).
- [7] M. Farizon, B. Farizon-Mazuy, N. V. de Castro Faria, and

H. Chermette, Chem. Phys. Lett. **177**, 451 (1991); M. Farizon, B. Farizon-Mazuy, and H. Chermette, J. Chem. Phys. (to be published).

- [8] W. Brandt, *Atomic Collisions in Solids* (Plenum, New York, 1975), Vol. 1, p. 261.
- [9] W. Brandt and M. Kitagawa, Phys. Rev. B **25**, 5631 (1982).
- [10] B. S. Yarlagadda, J. E. Robinson, and W. Brandt, Phys. Rev. B **17**, 3473 (1978).
- [11] P. Sigmund and K. B. Winterbon, Nucl. Instrum. Methods **119**, 541 (1974).
- [12] Yu. V. Kononets, Nucl. Instrum. Methods B **33**, 174 (1988).
- [13] N. R. Arista, Phys. Rev. B **18**, 1 (1978).
- [14] P. M. Echenique, R. H. Ritchie, and W. Brandt, Phys. Rev. B **20**, 2567 (1979).
- [15] Z. Vager and E. P. Kanter, Nucl. Instrum. Methods B **39**, 98 (1988).
- [16] J. C. Eckardt, G. Lautschner, N. R. Arista, and R. A. Baragiola, J. Phys. C **11**, L851 (1978).

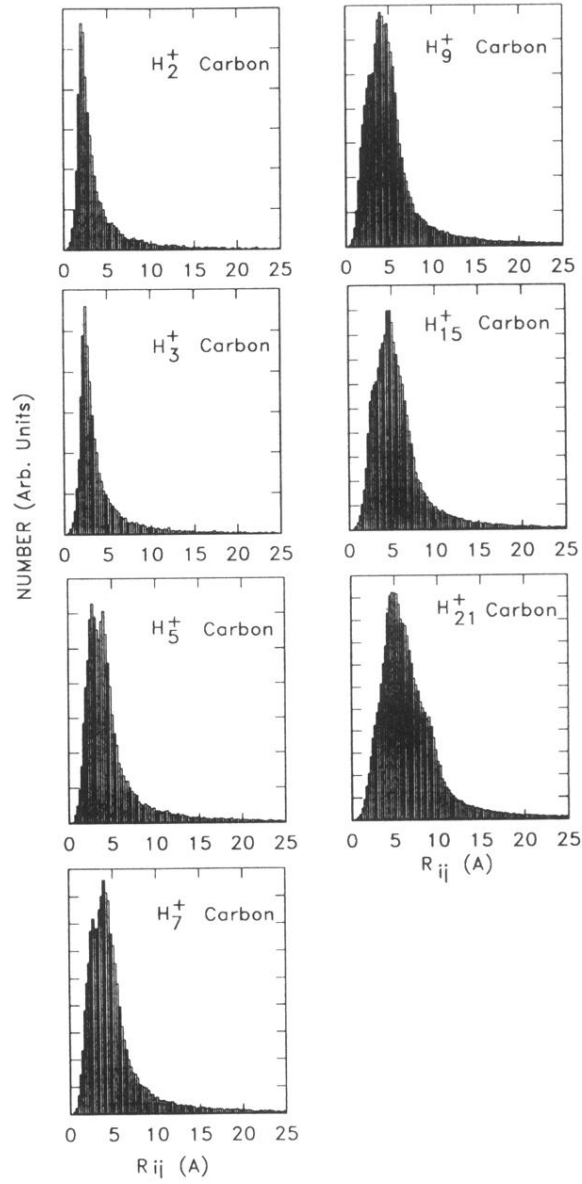


FIG. 5. Calculated internuclear separation distributions  $F(R_{ij})$  resulting from the passage of 60-keV/p  $H_n^+$  clusters ( $n=2,3$  to 21, odd) through 1  $\mu\text{g}/\text{cm}^2$  carbon foil.